RECORD – MAIN S&T RESULTS / FOREGROUNDS

1. WP1

1.1. Objectives and limitations of WP1

WP1's objective was to study the canonical case of indirect noise generation: the passage of an entropy wave through a nozzle. In addition, other excitation means were tested (vorticity waves for example). The goal was to verify weather low order models were able to reproduce the experimental data but also to investigate this case in more details using high fidelity simulations.
Two configurations were tested: EWG and HAT. DLR performed the experiment in both EWG and HAT cases. Most simulations were performed for the EWG cases which proved sufficient to capture most of the phenomena. UCAM and FFT performed low-order simulations of entropy waves passing through the nozzle. LES was used by CERFACS in RECORD for the computation of the subsonic test case RECORD_WP1_EWG_2 of the Entropy Wave Generator test rig. The objective of LES was to go one step beyond zero-dimensional tools which have been studied up to now and also developed during WP1 by UCAM and FFT.

1.2. Target experiments

In WP1, two setups were proposed by DLR: EWG and HAT. Depending on what the simulation teams wanted to do, they used one or the other.
The Entropy Wave Generator test rig facility at the German Aerospace Centre (DLR) simulation by means of a full 360 Large Eddy Simulation (LES) will be described. The selected test case to be computed with the numerical code AVBP (T. Schonfeld (1999)) is a subsonic case with a nozzle Mach number of 0.7 (test case RECORD_WP1_EWG_2). A sketch of the EWG test rig is shown in Figure 1 and Table 1 summarises the different elements positions.

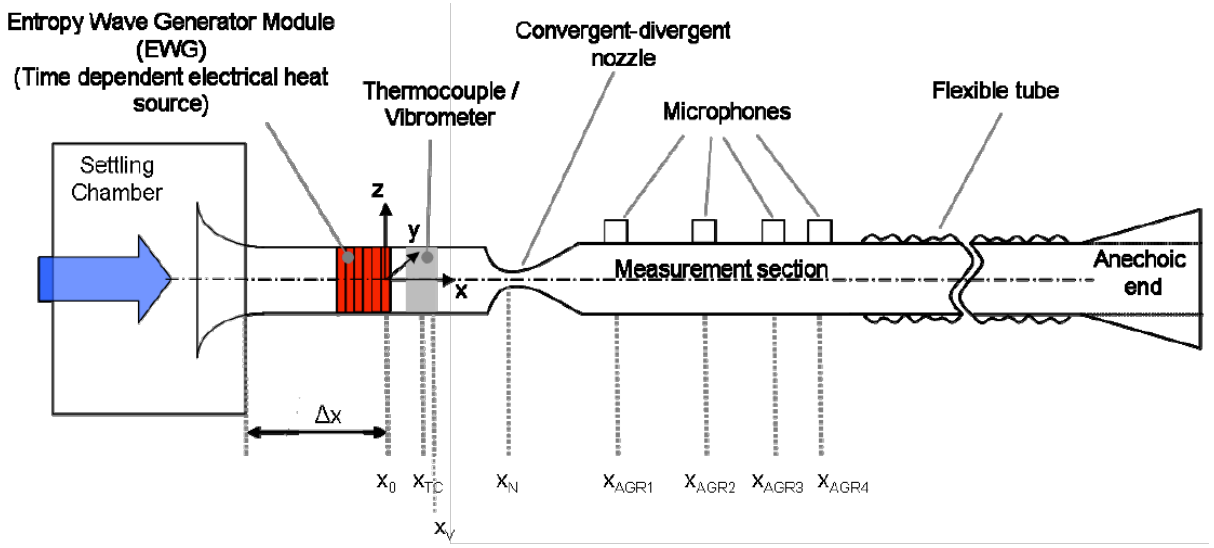

Figure 1 Sketch of the EWG experiment and position of different elements

Element	Acronym	Distance from nozzle (mm)
Upstream heating ring	X_0	-105.5
Thermocouple	x_{TC}	-72.5
Vibrometer	x_V	-58
Nozzle throat	x_N	0
Microphone 1	x_{AGR1}	350.5
Microphone 2	x_{AGR2}	730.5
Microphone 3	x_{AGR3}	975.5
Microphone 4	x_{AGR4}	1150.5

Table 1 Summary of the positions of different elements of the EWG rig

Different configurations of numerical parameters and grids have been tested to make these simulations be representative of the experiment. The test case simulated by CERFACS corresponded to the case number two described by F. Bake et al. (2009). A summary of the different parameters of the flow and forcing are discribed in Table 2.

The first studies were addressed to study if the tranquilisation chamber has to be computed and if the flow separates in the nozzle. Hence, different parameters where assessed: geometry (entire or simplified), numerical schemes and the LES models.

Parameter	Value
Mass flow rate (kg/h)	37
Nozzle Mach number	0.7
Pressure (settling chamber; between honeycomb flow straightener and tube inlet) (Pa)	105640
Nozzle pressure (Pa)	68650
Mean flow velocity in the upstream tube (m/s)	11.39
Pulse duration (ms)	100
Electrical heating power (W)	192.7
Thermal heating power (W)	138.2
Temperature increase (K)	13.4
Heated wire rings (no. 1 is the must upstream ring) delayed according to flow velocity	1-6

Table 2 Parameters concerning the flow and the excitation conditions of the EWG reference test case 2

The second setup used in WP1 is the HAT which was also operated at DLR and extended the cases tested in the EWG setup.
The test duct of the HAT rig (Figure 2) has an inner diameter of 70 mm and a total length of about 5.4 m. It consists of two symmetric measurement sections with the nozzle / liner module in-between and anechoic terminations at both ends. A loudspeaker (A and B) is mounted at the outer end of each measurement section. Microphone probes can be installed at ten axial positions upstream and downstream of the nozzle / liner. Some of the microphone probes in the upstream section were removed for the experiments with entropy spots for the installation of injection tubes.

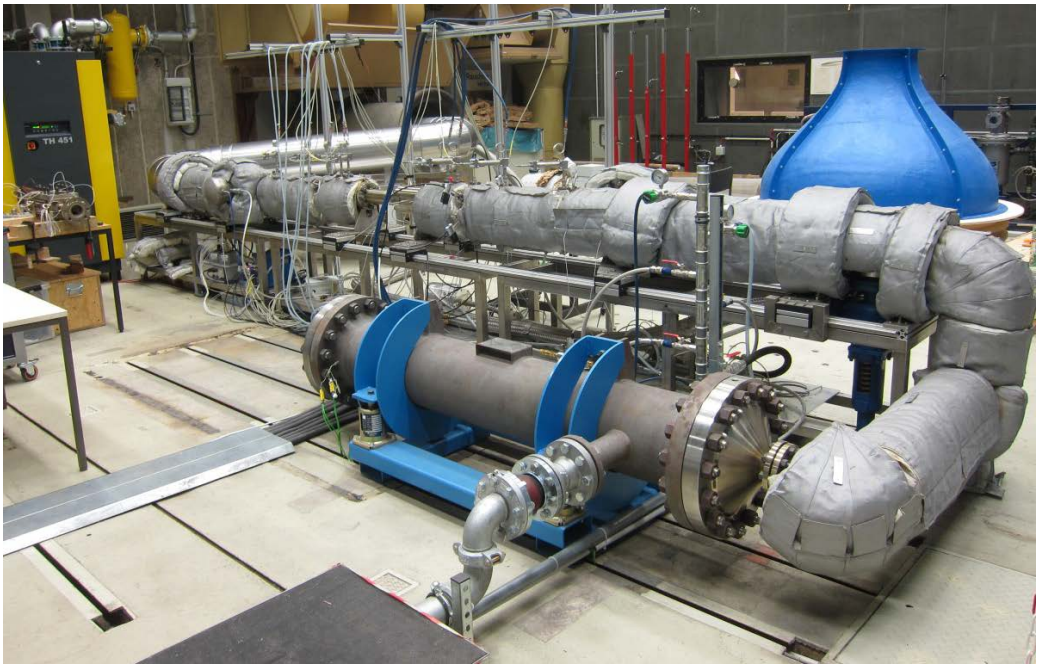

Figure 2: Overview of the HAT facility with the nozzle module installed.

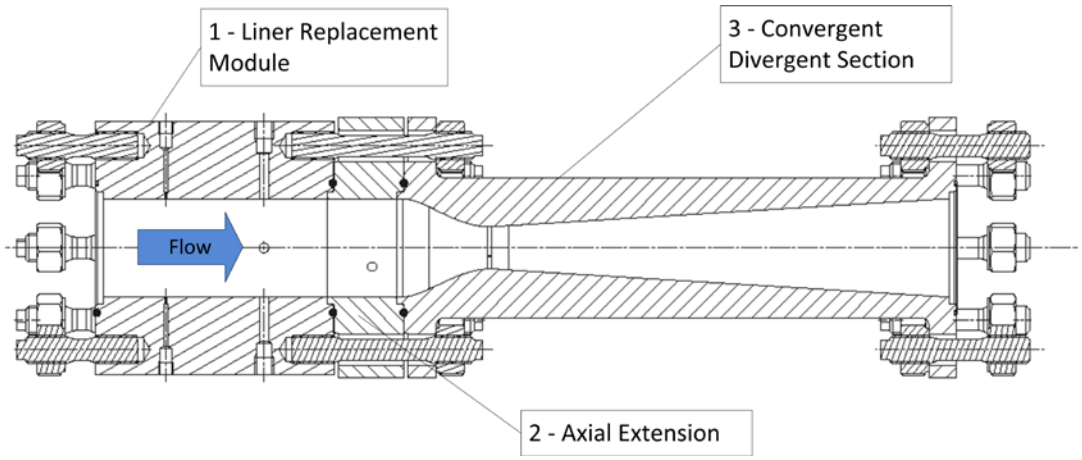

Figure 3: Nozzle Module with Liner Replacement module (used for test cases HAT_1 and HAT_2)

Two different ways of excitation were investigated:

- By means of two loud-speakers, the acoustic characteristics of the nozzle module were investigated in the plane wave regime for frequencies between 200 and 2800 Hz (upper limit corresponds to the cut-on frequency for higher order modes at ambient temperature). While a first test case (HAT_1) investigates the acoustic transmission and reflection of the nozzle module itself, a second test case (HAT_3) includes a bias flow liner for the effective damping of acoustic pressure fluctuations.
- Entropy forcing was accomplished injecting cold air into the hot mean flow. Test case HAT_2 exhibits additional pressure fluctuations (noise) when cold spots are entering the nozzle. For test case HAT_4, the bias flow liner was installed downstream of the cold flow injection aiming at a reduction of temperature/entropy gradients and thereby reducing the additional noise source.

1.3. Main results

All objectives of the initial WP1 program have been achieved in a reasonable manner. DLR has been able to produce a large data base providing all information on EWG as well as HAT runs as planned in the technical annex of RECORD. UCAM and FFT have applied their low-order tools to these cases (mostly EWG but also HAT data) and CERFACS has performed a full LES of the EWG setup and should finish a HAT case before the end of 2015.

Overall conclusions are the following:

- Even though great care was taken experimentally to control acoustic reflections, these phenomena still affect slightly the pressure traces used for indirect noise assessment in the nozzle exit. As found a few years ago by other groups (DLR or CERFACS), some description of acoustic reflection at inlet and outlet is required in the low order models for example at the outlet to mimic the pressure signal measured at DLR.
- The low-order models LOTAN and ACTRAN are able to recover the pressure traces measured experimentally with reasonable precision and limited tuning. LOTAN (the Cambridge code) seems to produce more accurate results than ACTRAN (the FFT solver).
- LES performed at CERFACS shows that the flow details (the distribution of the heat source terms, the 3D flow velocity profiles, especially near the throat) modify slightly the results but that the 1D approximations used in LOTAN or ACTRAN remain reasonable. Moreover, since the flow is turbulent, LES data must be cycle-averaged over many realisations to eliminate turbulent noise from the pressure signal in the nozzle exit section.
- Control strategies for indirect noise were also tested by DLR, using bias flow to mitigate entropy waves and therefore indirect noise.
- The scattering matrices computed by TUM showed good agreement with analytical models and experiments in the case of the EWG and HAT, respectively.
- The indirect noise generation by entropy (EWG) and vorticity waves (VWG) is captured by the RANS/LNSE approach and delivered consistent results with experiments.

1.4. Conclusions

WP1 was a prerequisite step in RECORD: being able to compute the generation of indirect noise in a simple nozzle flow was required to address the more complex cases of WP2, 3 and 4 which all feature geometries with area variations but also many other complex physical phenomena (combustion for WP2, rotating parts in WP3, real systems in WP4). The WP1 overall conclusion is that even though LES results indicate a few limitations related to the assumptions required handling the problem in low-order formulations, those are minor issues compared to other questions such as the existence of acoustic reflections at inlet or outlet. The general result is that using the low-order models for the other RECORD work packages is a reasonable approach which is being pursued now for WP2 and WP4. Note also that LES will also be applied in the other work packages to bring other information for low-order modelling and for general descriptions of the physics.

2. WP2

2.1. Recall of the objectives of WP2

The present part of the project addressed the question of noise sources caused by combustion. The source identification remains a critical issue and experimental data are necessary to test and validate different modelling strategies. The discrimination of direct and indirect noise emitted by the flame under various conditions was envisaged from experimental as well as numerical points of view. A well-controlled lab-scale configuration was designed to contain the major physical processes encountered in GT combustion chambers. On the numerical side four different types of numerical tools, with different levels of fidelity, were envisaged. Efforts focused on the analysis of flame dynamics to determine acoustic sources in the flame environment. The main objectives were:

1. To build comprehensive sets of experimental data to be provided to the partners, for high fidelity as well as low-order model validations.
2. To assess the capacities of state-of-the-art numerical tools to evaluate both noise sources and transmission.
3. To improve the numerical tools.

The experimental activity and the development of the four simulation tools associated with four levels of fidelity constitute the five first tasks of WP2 (WP2.1 to WP2.5), which ends with the data appraisal activity (WP2.6), finally involving all the WP2 partners: AVIO, CERFACS, CNRS, ONERA, RRD, RRUK, TM, TUD, TUM, UCAM.

2.2. Specifications

Originally, the specifications were defined with all the partners in the report associated with the milestone M2.1 “Test readiness review. Definition of test matrix for simulations”, uploaded on the PDES. However, during ignition and operation procedures, a consequent variety of issues were encountered with the original two-stage configuration, which were highly disturbing in terms of safety and robustness. Due to these issues, crucial scientific questions could not be tackled. The addition of air and fuel by the so-called first stage strongly contributed to the development of these issues. This motivated a meeting with all the partners involved in WP2, which was held on November 27th 2014 at CNRS/EM2C. We proposed to modify the injection system by removing the 1st stage, keeping the 2nd stage identical (Figure 2). We strongly recommended changing towards the proposed new injection design and to abandon the original two-stage one. All the WP2 partners present at the WP2 meeting unanimously accepted this recommendation. Moreover, following TUM’s advice, it was decided to include a high-speed jet in the centre of the upstream ICS, increasing the degrees of freedom of the combustor.

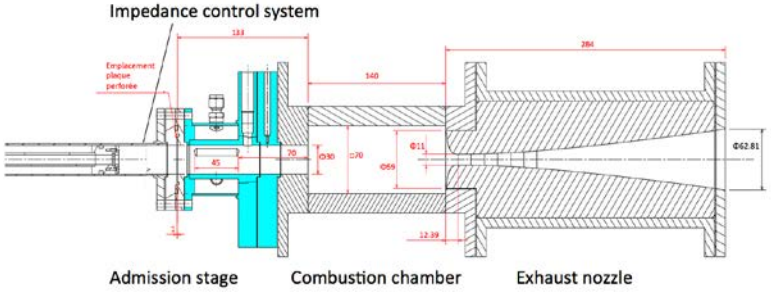

Figure 4: Modified configuration of the Combustor

(a) 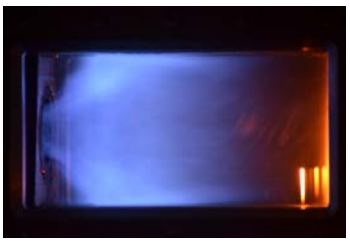 (b) 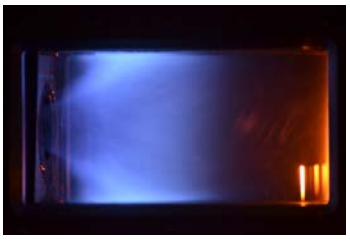

Figure 5: Natural emission of flames in three distinct regimes using the modified configuration. Φ = 0.85. (a) OP1: m_{a2} = 13 g/s, m_{ax} = 5 g/s, (b) OP2: m_{a2} = 16 g/s, m_{ax} = 2 g/s,

Final specifications for operating points

Global parameters remain constant: Air mass flow rate: 18 g/s; Φ: 0.85.
3 final configurations:

- OP1: 16 g/s main, 0 g/s jet, 2 g/s piston (reference point, see Figure 3(b)).
- OP2: 16 g/s main 2 g/s jet, 0 g/s piston
- OP3: 13 g/s main, 5 g/s jet, 0 g/s piston

2.3. Experimental results

The main objectives were as follows:

- To provide systematic sets of data to the partners for validation of their developments
- To identify and analyse direct and indirect noise contributions

The main achievements are the following ones:

- We characterized the aerodynamics and combustion processes
- We studied the influence of boundary conditions on combustion noise
- We measured steady as well as unsteady temperatures in the combustion chamber
- We developed post-processing for dynamical analysis: direct and indirect contributions

All these elements were provided to the partners for comparison and validation of their own developments.
Temperature fluctuations were determined experimentally by LIV. Temperature fluctuations were shown to be dominated by low frequency dynamics with slightly higher levels for OP3b (13.4-4.6-0). To our knowledge this represents one of the first attempts to determine temperature fluctuations for such a large range of frequencies and in such a harsh environment. LIV measurements, combined with high-speed pressure measurements and plane wave decomposition allow separating direct and indirect combustion noise contributions (Figure 4). Measurements show that indirect combustion noise exists, but direct combustion noise is dominating. Results depend strongly on the test bench arrangements du to the high quantity of interactions between different phenomena. Work on CESAM-HP allowed to obtain a possible methodology to study direct and indirect combustion noise.

2.4. Compressible LES approach

The main objectives were as follows: To perform HFLES computations of the CNRS experiment; To provide systematic sets of data to the partners for comparison and validation.

The main achievements were the following ones:

- We performed (cold &) reacting flow simulations
- We improved our models and our numerical methods
- We evaluated the direct and indirect noise contributions from the simulations

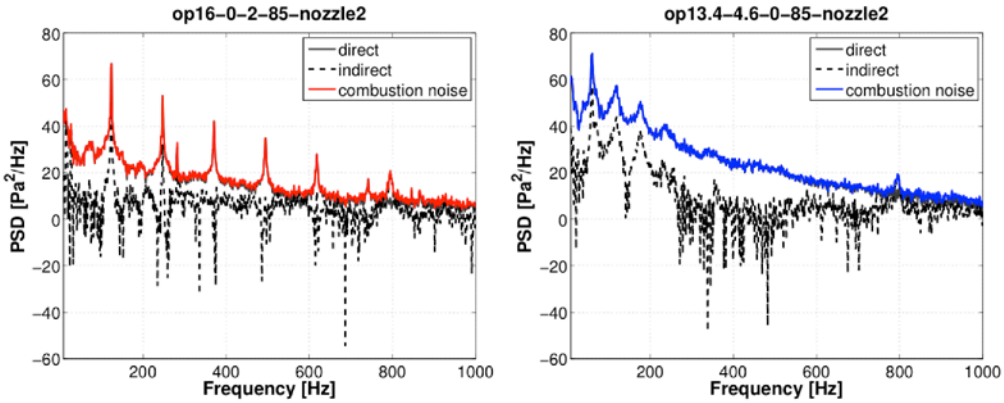

Figure 6: PSD of acoustic pressure in experiments. Direct and indirect contributions as extracted from the plane wave decomposition.

Operating point OP3 (13-5-0-85) is very close to unstable regimes, making its analysis on a combustion noise point of view rather difficult. In spite of that, the presence of a strong flame motion at low frequency (~ 100 Hz) was detected in both computations (Figure 5). It strongly affects the velocity mean profiles and increases the RMS levels. The 'n'-type CEDRE computations better fits the experiments for the mean velocity profiles but does not catch the low frequency motion. The 'b4n2'-type CEDRE calculations show a representative spectral content with little excess of low frequency oscillations leading to radial profiles with a high activity in the centre. Simulations performed with AVBP show good spectral content and Ux and RMS values at centreline but they present a different cone angle and lower values at higher radius. Finally the impedance at the ICS end was effective in controlling the low frequency motion. Overall comparisons were satisfactory and noise analysis could be performed. The two codes provided consistent results with different numerical ingredients.

HFLES computations demonstrated a very good accuracy in overall flow features; dynamic pressure time signal and PSD in the chamber; temperature data in the plenum. Both numerical chains proved good readiness level. Their application to the WP2 experiment yielded combustion noise sources evaluations that were in agreement with the experimental evaluations (Figure 6).

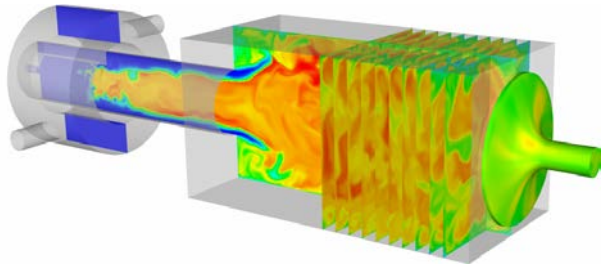

Figure 7: LES geometry and unsteady temperature field. Definition of planes used for the characteristic filtering using the Riemann invariants.

2.5. Uncompressible LES approach coupled with CAA

The main objectives were as follows:

- To predict direct combustion noise emission by a hybrid LES/CAA coupling approach
- To generate and propagate entropy waves, vorticity waves, and acoustic waves using coupled codes
- To implement acoustic feedback onto the flow or flame via appropriate model

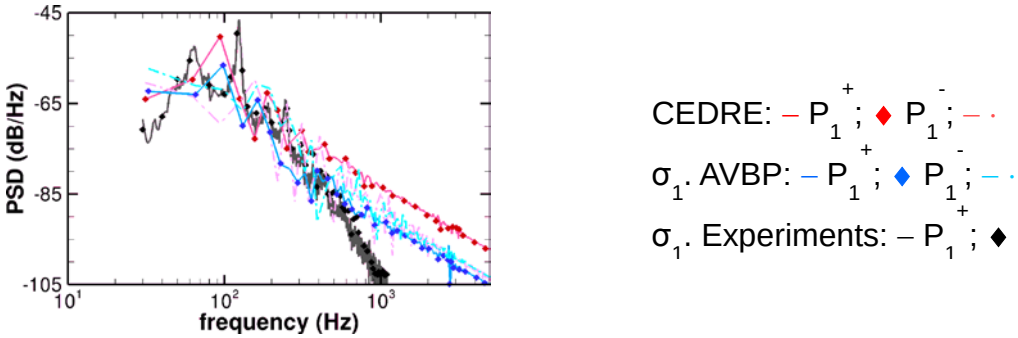

Figure 8: Power spectral densities of Riemann invariants in the experiments as well as in CEDRE and AVBP computations.

The main achievements were the following ones:

- We performed (cold &) reacting flow simulations using uncompressible LES
- We proposed an original code coupling methodology and validated the methodology
- We studied the impact of different input data on the results

The coupling between the CFD solver and the CAA code could be adjusted through spatial interpolation (CWIPI), spatial filtering and temporal interpolation. The validation of the whole coupling process was successful (Figure 9).

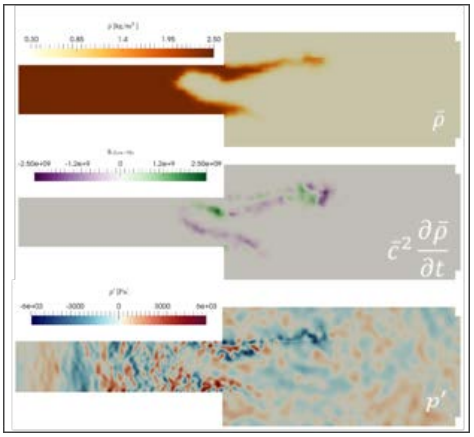

Figure 9: Illustration of the coupling process between the uncompressible CFD solver and the CAA code. Top: Mean density field. Middle: Noise sources as extracted from the CFD calculation. Bottom: acoustic pressure in the CAA solver.

2.6. RANS/LNSE simulations and Statistical Models

The main objectives were as follows: to perform steady reactive RANS in order to provide statistical inputs to the models; to validate the spectral combustion noise source model; to carry out calculations of the frequency spectra of the combustor pressure.

The main achievements were the following ones:

- We performed (cold &) reacting flow simulations using steady RANS
- We developed & assessed noise propagation methods
- We improved the statistical combustion noise source identification process
- We identified sources of combustion noise

The noise model accurately predicted the noise level and its trend for OP1 (16-2-0-85) and OP2 (16-0-2-85). In the case of OP3, a strongly unstable behaviour makes it extremely difficult to

converge the simulation and therefore to obtain relevant results for the noise propagation. Major improvements of the acoustic simulations were realized by the implementation of a flame transfer function. Quasi-2D and 3D model delivered comparable results, despite of the simplifications of the 2D model (Figure 7).

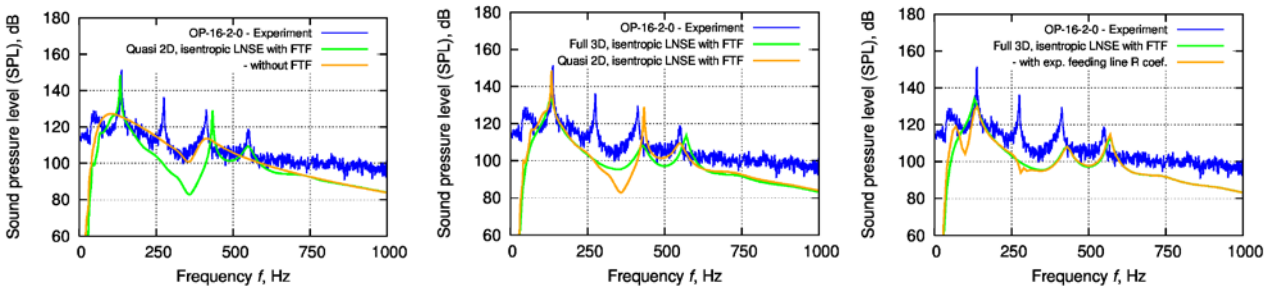

Figure 10: Sound Pressure Level in dB for the three parametric studies. Left: with and with out the FTF. Middle: Quasi-2D versus full 3D. Right: Influence of the feeding lines.

A highly efficient methodology is presented which significantly reduces the computation effort while delivering good agreement with experiments. This hybrid method can be used as a predesign tool.

2.7. Low-Order Model

The main objectives were as follows: to determine TFs between acoustic, entropic and vortical waves incident on a downstream choked nozzle and the unsteady heat release; to integrate the spectral combustion noise source model developed in Task 2.4.

The main achievements were the following ones:

- Post-processing of LES data
- Implementation of shape functions in the low-order code LOTAN
- Implementation of TUM model into LOTAN
- Calculations of pressure and entropy waves at the combustor exit

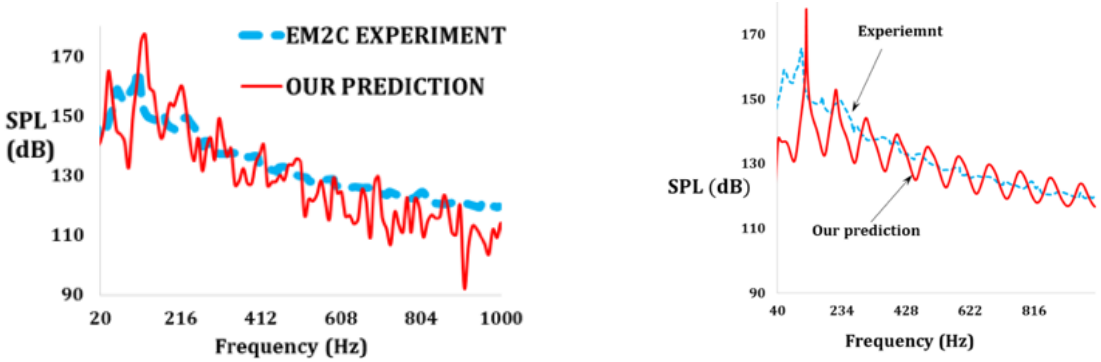

Figure 11: Left: Comparison between experimental (blue) and modelled sound pressure level (SPL) in dB. Right: Comparison between experimental (blue) and modelled sound pressure level (SPL) in dB.

The LOTAN in combination with compressible LES predicts very well the pressure spectra as measured in the experiments. LOTAN in combination with an extended version of spectral model of Hirsch et al. (2007) agrees reasonably well with the experimental data. For low frequencies the predicted pressure spectrum is about 20 dB less than that of the experiment. This is mainly due to the fact the heat release spectrum predicted by the model is one order of magnitude smaller than LES (Figure 8).

3. WP3

3.1. Introduction

The goal of WP3 was to investigate the generation of excess or indirect noise at a turbine and the transmission of direct noise through a turbine. For sake of simplicity the combustor is abstracted and only a single turbine stage is considered. The combustion process is replaced by controlled perturbations prescribed at the entrance of the turbine. Since there the mean inflow is axial and almost uniform (unless the hot streaks are simulated) the three perturbation types to be investigated (entropy, vorticity and sound) can be coupled clearly without ambiguity into the domain. The investigations were carried out with time-periodic perturbations of low to moderate amplitude which enabled the use of linearized frequency methods.

The experiments and simulations were thought of with the objective to investigate the following effects:

- indirect noise generation due to the interaction steady hot streaks with the turbine;
- indirect noise generation due to unsteady entropy spots passing the turbine;
- indirect noise generation due to the interaction of vortical structures with the turbine;
- reflection / transmission of acoustic waves through the turbine.

To achieve this objective a comprehensive test campaign was conducted at the PoliMi HPT test rig. This work was accompanied by numerical and analytical studies.

3.2. Turbine tests

The project had for objective to perform the test on a realistic turbine. The HPT rig available at PoliMi (see **Figure 12**) could comply with most of the specifications. The turbine is composed of a single HPT stator—rotor stage and is operated at atmospheric conditions. The combustor rig was abstracted and the incoming disturbances were generated either by an EGW/VWG device or loudspeakers placed upstream of the turbine. The rig was amply modified to comply with the specifications and receive the instrumentation.

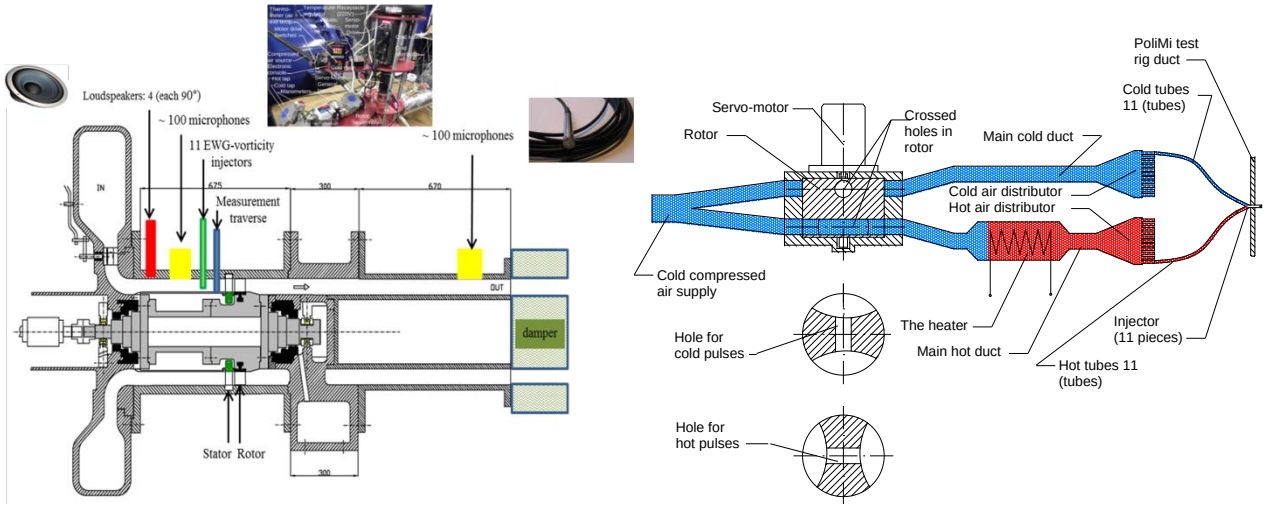

Figure 12: (left) Longitudinal cut of the PoliMi turbine rig with the position of the instrumentation; (right) EWG/VWG concept designed by SMCFPA to produce 35°C temperature pulses for 11 injectors.

The design and manufacturing of the EWG/VWG device to create the entropy and vorticity waves in the turbine environment was one of the main challenges of the tests. The working principle of the solution proposed by SMCPFA is sketched in **Figure 12**. The air flow supplied at ambient temperature is divided into two main streams, with one of these been heated using an electrical heater with 4.5 kW maximal power. The alternating flow is created by a rotating valve.

PoliMi was able to characterise the rig with respect to its main flow properties and aerodynamic performance. The results were used by the low-order models and also helped to validate the CFD calculations. The disturbances created by the EWG/VWG were also characterised with respect to total temperature and total pressure measured at the exit of one of the 11 injectors. These data were imposed as boundary conditions in the CAA calculations.

Two phased-microphone arrays designed by DLR with respectively 96 and 120 microphones were installed in the inlet and outlet sections of the turbine. These arrays were designed to properly decompose the acoustic field in azimuthal and radial mode orders up to the BPF frequency.

3.3. Turbine tone prediction

A CAA benchmark was conducted on the isolated turbine (without inflow perturbation). All the partners used a URANS type approach but different variants were applied (see **Table 3**).

	numerical approach	numerical scheme	turbulence model	type of BCs	number of cells	acoustic post-processing	acoustic eigensolution
UniFi	TL-FD	2^{nd} order	$k-\omega$	3D NRBCs	$\approx 7.0\times10^6$	RMA*	numerically solved
GE Avio	TL-FD	2^{nd} order	$k-\omega$	3D NRBCs	$\approx 6.0\times10^6$	RMA*	numerically solved
ITP	TL-FD	2^{nd} order	$k-\omega$	2D NRBCs	$\approx 8.2\times10^6$	RMA*	numerically solved
DLR	NL-FD	2^{nd} order	$k-\omega$	2D NRBCs	$\approx 7.0\times10^6$	XTPP†	Bessel functions
UPM	NL-TD	2^{nd} order	$k-\omega$	1D NRBCs	$\approx 3.0\times10^6$	RMA*	numerically solved
TM	NL-TD	2^{nd} order	$k-l$	characteristics	$\approx 9.6\times10^6$	surface integration	none

(fitted variables: * all primitives variables, † pressure only)

Table 3: Numerical strategies employed in the benchmark.

The results of this Benchmark were published in a joint paper presented at the ASME Turbo Expo 2015 Conference in Montreal (Canada). This benchmark ended before the tests were started. The global aerodynamic performance parameters of the turbine agree within less than 2% between the six partners. For the fundamental BPF the sound power level agrees within less than 3 dB if wave splitting methods are used for the acoustic post-processing.

Some of the partners involved in the numerical simulations were able to re-compute the reference operating point in order to better match the condition encountered during the tests. They obtained a very good agreement with the aerodynamic and acoustic measurements (see **Figure 13**).

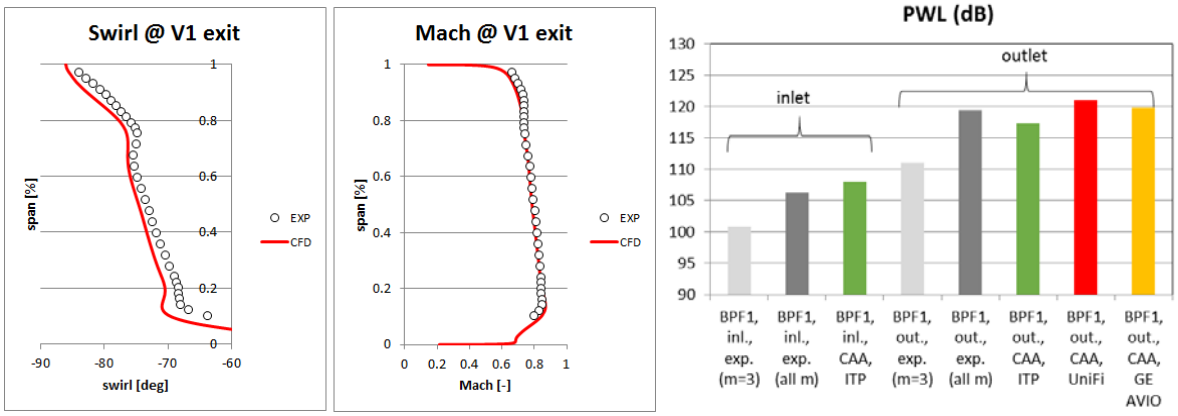

Figure 13: (left) Span-wise distributions of flow Mach number and swirl angle at stator exit; pitch-wise averaged results calculated by GE AVIO; (right) comparison between the acoustic levels of turbine tones measured exp. and calculated with CAA.

3.4. Steady hot streaks

The naming “steady hot streaks” denote the time-averaged or steady part of the combustion flow. DLR performed a parameter study with pure temperature spots imposed at the turbine entry while UniFi matched the experimental conditions. Both partners observed that the hot streaks cool down due to the fact that the flow is accelerated through the stator. This contributes to reduce the temperature ratio $\Delta T/T_{mean}$ at the stator exit. Another consequence is the increase of the speed in the streak region so that actually both the temperature and the vorticity fields are non-uniform at the rotor entry.

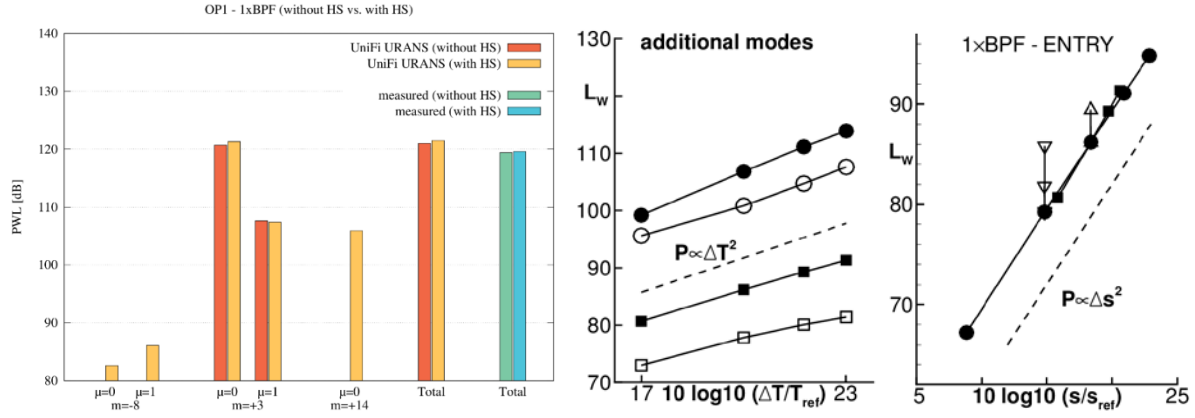

Figure 14: (left) UniFi results obtained with URANS; (right) PWL variation for the extra modes created by the streaks as a function of the hot streak temperature and entropy flow (DLR).

Both partners predicted only a little impact of the steady hot streaks on total tonal noise which confirmed the experimental observations (see **Figure 14**). Additional acoustic modes are produced by the interaction of the hot streaks with the turbine stage. The DLR results obtained with the Harmonic Balance technique indicate that the power amplitude associated to the additional modes increases with the square of the temperature difference and the fourth power of the diameter. With respect to entropy flow, the increase is to the square (as also predicted by Marble and Candel).

3.5. Entropy waves

Here a low frequency temperature variation was imposed at the turbine entry. Using the PoliMi measurements as input UniFi (URANS) and ITP (time-linearised method) were able to obtain results in excellent agreement with the experiment (see Figure 15).

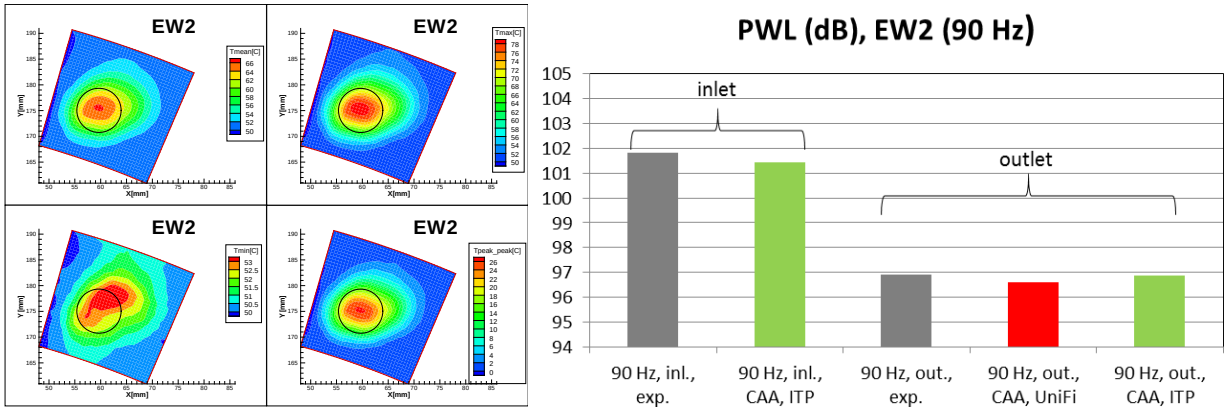

Figure 15: (left) Temperature variations measured by PoliMi; (right) Comparison between the acoustic power levels measured exp. and calculated by CAA.

The results presented in **Figure 16** were obtained by UCAM with LINEARB, a code implementing a low order model similar to that presented by Cumpsty and Marble (1977). The results with entropy waves imposed at the turbine entry (left hand-side graph) indicate that the entropy noise in the gap between two blades is the dominant source in production of sound at the turbine outlet. This result suggests that entropy indirect noise measured downstream the turbine is mainly created by the entropy spots as them pass though the rotor. The comparision of the level at BPF to that of the reference test case without prescribed entropy disturbance shows that the impact of the low-frequency low amplitude entropic waves on the turbine tones is negligible.

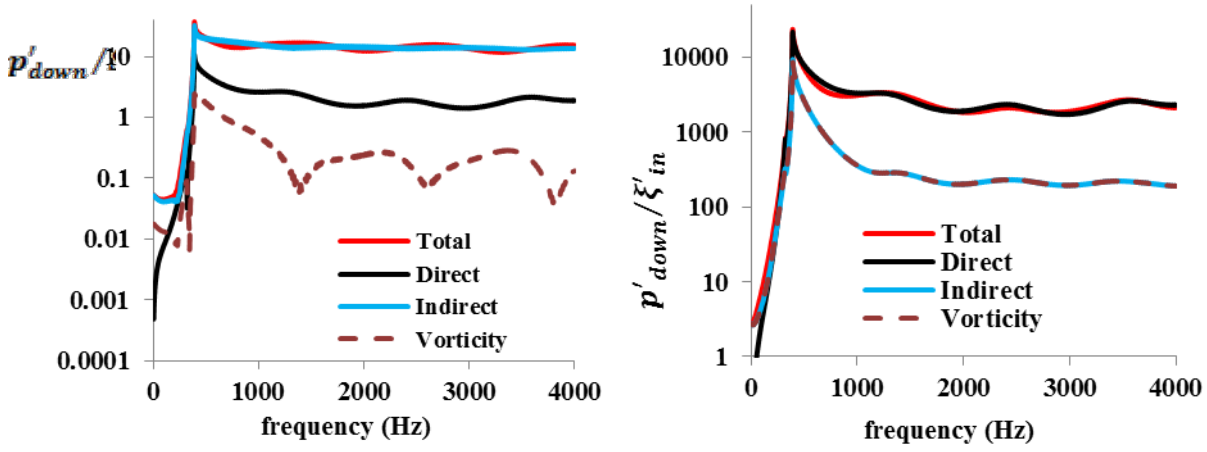

Figure 16: Variation of pressure wave downstream of the rotor due to acoustic wave (black line), vorticity (dashed brown), entropy + vorticity or indirect (blue line) and total (red line) in the gap between stator and rotor as a function of frequency predicted by incoming (left) entropy and (right) vorticity wave with azimuthal order m=1.

3.6. Vorticity waves

For an incoming vorticity wave interacting with the stator, LINEARB predictions support the idea that the acoustic wave generated at the stator is the main mechanism of noise generation at the turbine exit (see right graph of **Figure 16**). Although for $m \geq 1$ at frequencies close to cut-off frequency the vorticity wave interaction with the rotor can also be important. **Figure 17** shows the CAA results of ITP, GE AVIO and UniFi. The acoustic generation at the pulsation frequencies (30 Hz or 90 Hz) show a mismatch of up to 5 dB compared to the measurements. This mismatch may be due to the presence of high downstream running acoustic waves at the stage inlet where a non-anechoic termination is present. It is worth noticing that the acoustic power at the pulsation frequency is two orders of magnitude lower than the BPF turbine tone.

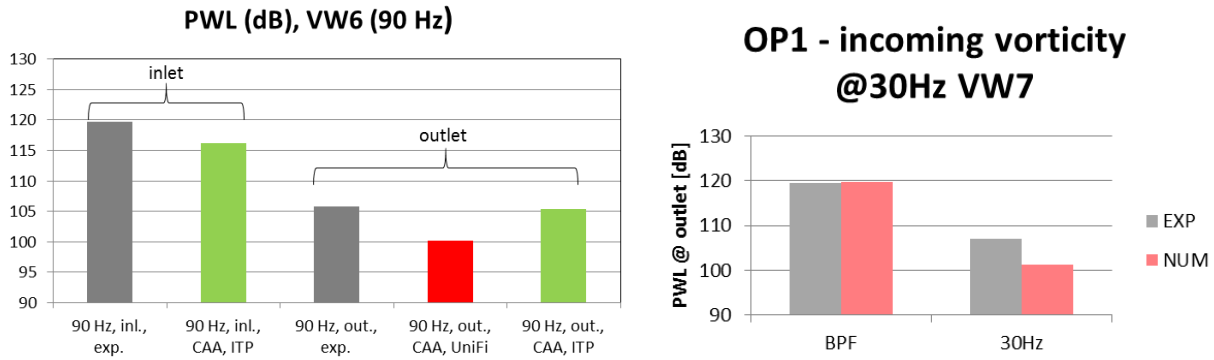

Figure 17: Comparison between the acoustic power levels measured exp. and calculated with CAA.

UPM has synthetized a new test case by combining the total temperature and total pressure distortions of two tests corresponding respectively to an entropy and a vorticity wave experiment at 90 Hz. **Figure 18** shows the axial evolution of the computed acoustic power levels calculated along the stage. The CAA results are in agreement with the experimental results even though the levels do not perfectly match. They show that the acoustic level increased by almost 7 dB in the outlet section but only by 2.2 dB in the inlet section when entropy is added.

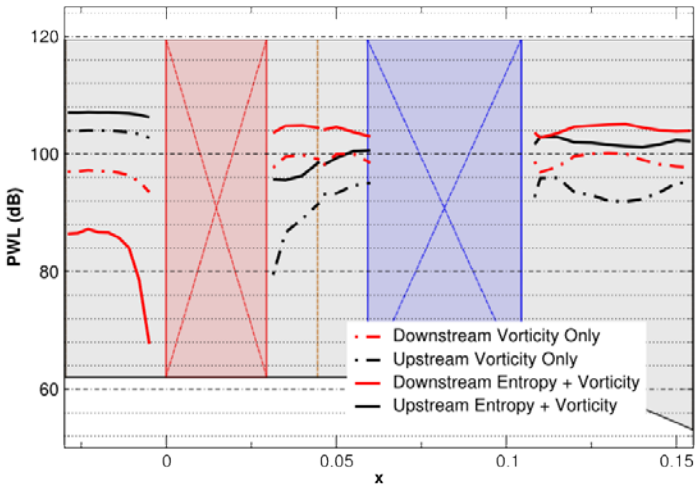

Figure 18: Radiated sound power level across the stage as simulated by UPM.

3.7. Acoustic waves

The last investigation concerns the transmission / reflection of acoustic waves through/by the turbine. A good qualitative agreement is obtained between the LOM, CAA and experimental results in terms of both transmission and reflection coefficients (see **Figure 19**). The numerical predictions confirm the acoustic behaviours highlighted during the test campaign, and in particular verify that the summation between transmitted and reflected power is not equal to 100% of the imposed acoustic power. Therefore the main conclusion, not necessarily general but for sure applicable to the RECORD test case, is that direct noise can be strongly dissipated by the turbine. A possible explanation for this is the conversion of the incident acoustic power into vortical perturbations. There is also a strong reflection of the incoming waves which results into low transmission coefficients whose values barely reach 10%. The partners also compared the impact of the spinning direction on the transmission and reflection of the mode |m| = 1. All results indicate a difference to the plane wave case. The difference is more or less significant and unfortunately all trends are not similar. On transmission, the experimental and GE AVIO simulation results indicate that the mode m = 1 (co-rotating with respect to the rotor) is less transmitted than m = -1 (contra-rotating). DLR, UCAM and TM results show the opposite trend.

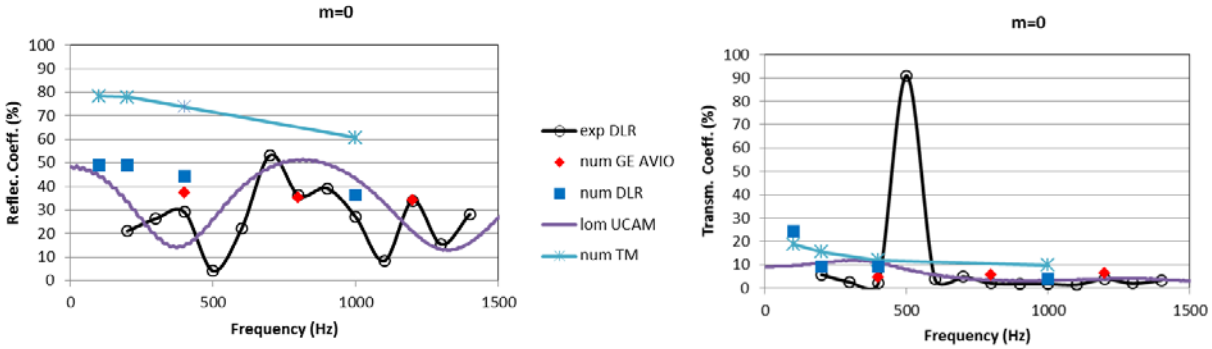

Figure 19: Reflection and transmission coefficients for the azimuthal mode order m = 0.

The strategy followed by FFT consisted in coupling the low-order model proposed by Cumpsty and Marble to two propagation sections (here two annular ducts) located upstream and downstream of the turbine. Thus it becomes to account for complex effects including e.g. the acoustic damping by a liner or modal scattering in the transmission of acoustic waves.

4. WP4

WP4 enabled innovative methods, brand new or fine-tuned within RECORD, to be successfully applied to full-scale industrial test cases and compared to experimental results (where already available).

RRUK / UCAM manage to predict the combustion noise spectrum at the exit of a demonstrator aero-engine.
Based on both mean and statistical flow data from the RANS calculation (provided by RRUK), a source model and the LOTAN code are used at UCAM to predict the broadband spectrum of fluctuations within the combustor. Then, LINEARB code is used to study the propagation of direct combustion noise and generation of indirect combustion noise through the turbine blade rows.
The schematic view of combustor and turbine of the demonstrator used for this comparison is following.

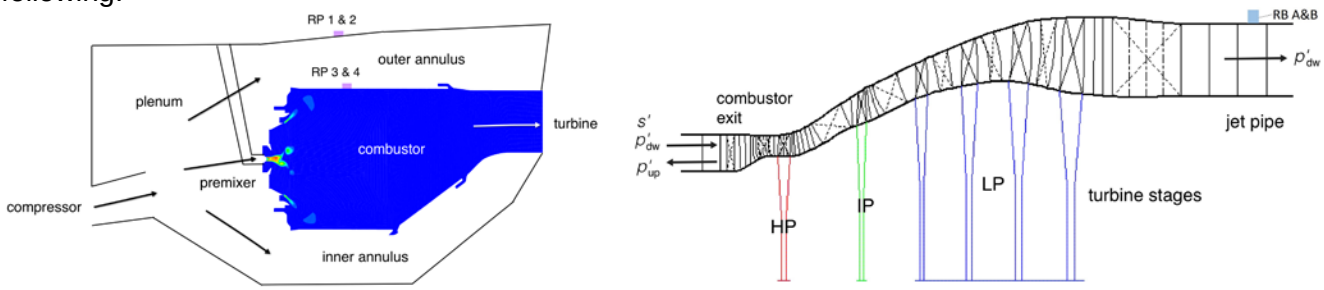

Schematic configuration of the demonstrator engine combustor (left) and turbine (right), with RP1 to, RBA and RBB rumble probes indicated.

Main Results

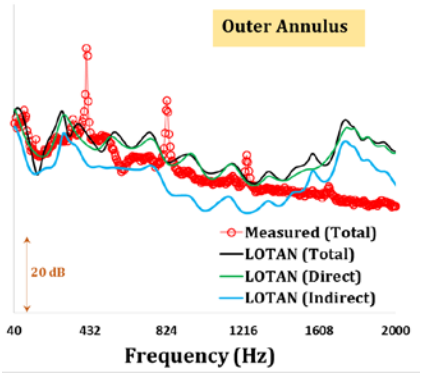

(a) SPL comparison on RP1 probe

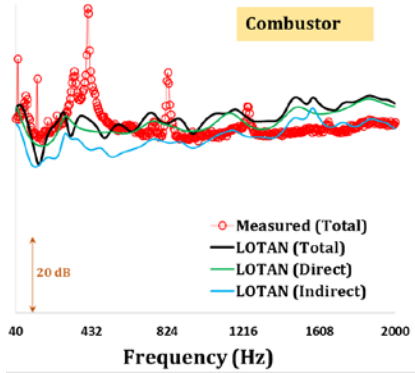

(b) SPL comparison on RP3 probe

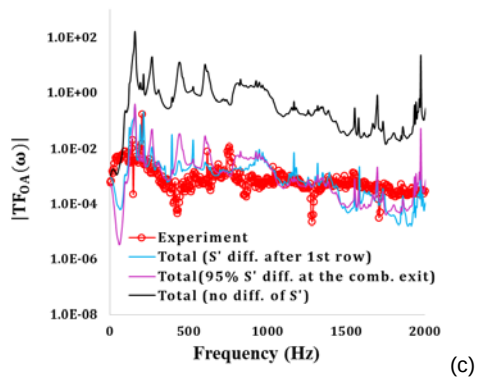

(c) Comparaison in jet pipe, several adjustments considered

A very good agreement between predictions and experimental data (a, b) is found inside the combustor where direct combustion noise is dominant. Application of rough LOTAN code through the turbine (c) shows a dominant indirect combustion noise component well above experimental results at the end of jet pipe. Several ponderations were studied, justified by the fact that LOTAN do not include yet entropy diffusion and dispersion effects.
It is seen that **when the attenuation of the entropy wave is included the total noise predicted is in good agreement with the experimental data in jet pipe, which seems dominated by indirect combustion noise**. Although for low frequencies (f<100Hz) the calculated results are much lower than experimental data.

TM / CERFACS tried to predict the combustion noise spectrum of a turboshaft helicopter engine in the far field.
The interest of a helicopter engine with respect to turbofan engines is that outlet mean flow is so low that jet noise is almost negligible, which means that experimental data, even in far field, is closer to "pure" combustion noise than for other kind of aero-engines. This does not mean that other noise sources, such as broadband turbine noise, cannot be present!
The CONOCHAIN methodology has been developed by CERFACS in the frame of this project and compared to the Ardiden engine database from the TEENI project (2008-2013).

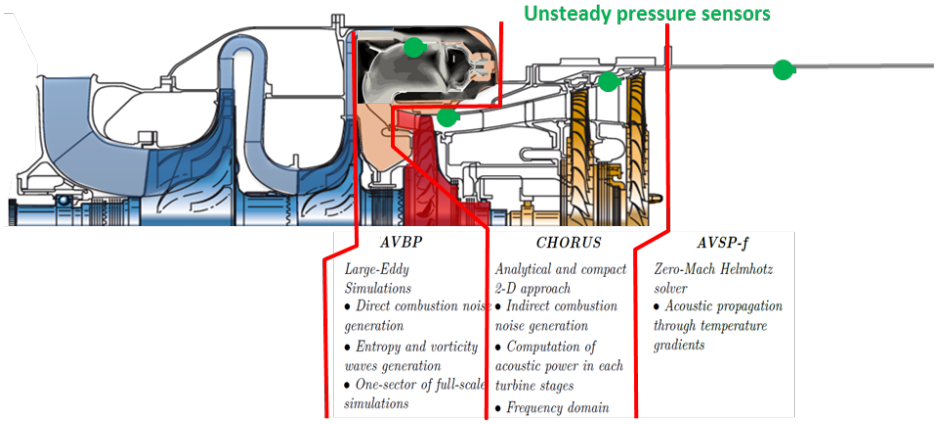

Application of the CONOCHAIN methodology to the Ardiden engine as used in the TEENI project, with internal instrumentation.

Main Results

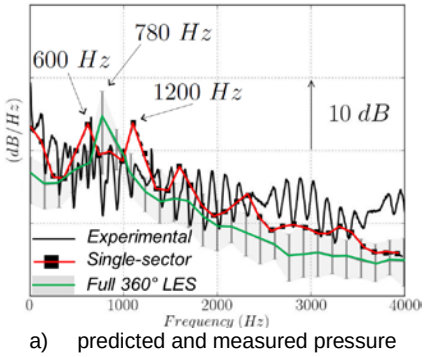

a) predicted and measured pressure spectra in combustor

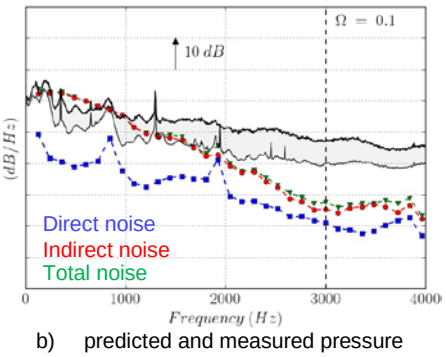

b) predicted and measured pressure spectra in nozzle

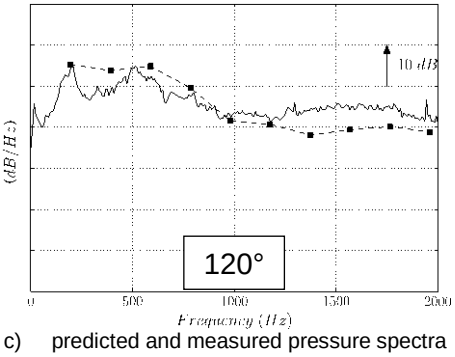

c) predicted and measured pressure spectra in far field

Very good agreement with experiment is found inside the combustor from AVBP results only (a), for both one sector and full 360° computations, where direct combustion noise dominates. A methodology has been achieved to continue exploiting one-sector computation which are current combustor design standard at TM.
Measured and computed spectra are also very similar in the frequency band of interest after the turbine (CHORUS (b)) and in the far field around the maximum of radiation (AVSP-f (c)), while some important differences are observed around 90° and 180°, probably due to the assumptions in the radiation model. **Computed combustion indirect noise dominates over combustion direct noise.**

GE-AVIO / TUM wanted to predict the combustion noise spectrum at the exit of the KIAI combustor test rig and apply this methodology to full-scale combustor from the NEWAC demonstrator.

A stationary RANS calculation is performed, and is post-processed in order to obtain a spectrum of heat release. This acts as the noise source of the acoustic problem, solved using Linearised NS solver on a quasi 2D and a full 3D meshes.

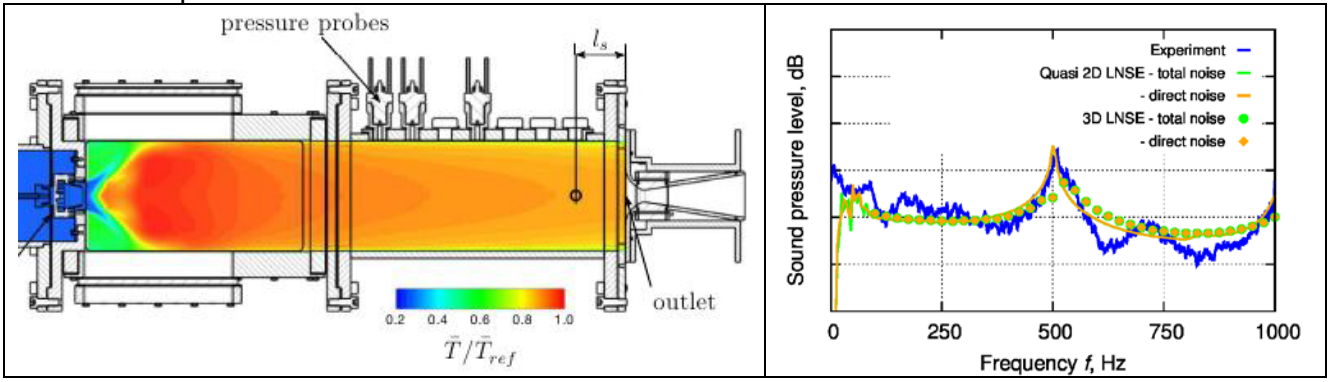

Good agreement has been met between calculated and experimental data. Direct noise is dominant inside the combustor.

After this validation exercise, GE-AVIO / TUM applied the same methodology to the combustor of the NEWAC demonstrator for noise evaluation purpose, using two different models with different levels of simplifications.

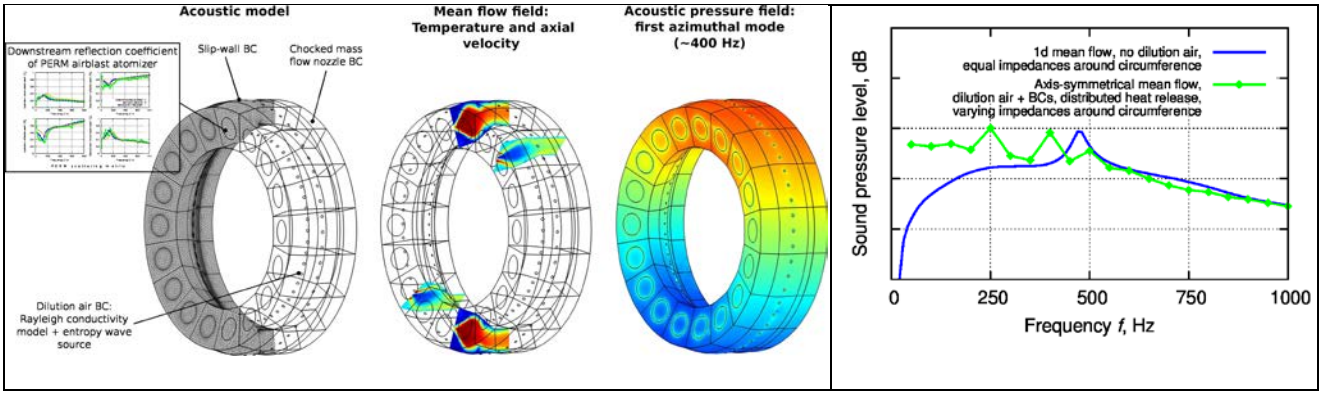

Unfortunately, no experimental data is available for comparison with this calculation at this point in time. Next steps on this model are to include a more realistic mean flow field and boundary conditions.

SN / CERFACS have predicted the combustion noise spectrum and directivity of an aero-engine in the far field. The CONOCHAIN methodology has been applied, using a one sector geometry representation in AVBP..

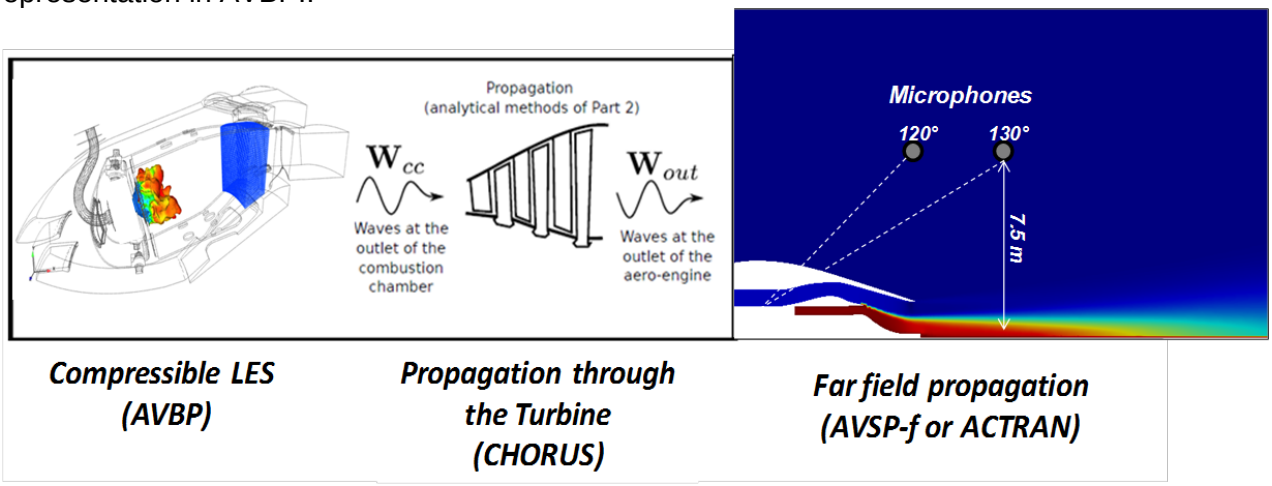

Main Results

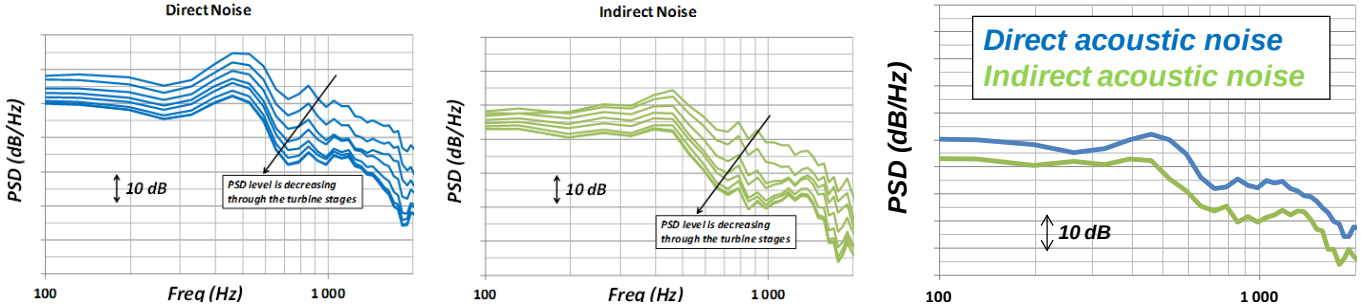

The shape of the spectrum is globally kept through the transmission process for both DCN and ICN-s', even if high frequencies are more attenuated than the lower ones. The calculations show acoustic power losses around 2dB per blade rig depending on the stage, a bit more for the first stages and a bit less for the lasts stages.
DCN is clearly dominating versus ICN-s'. ICN-w' is found almost negligible.

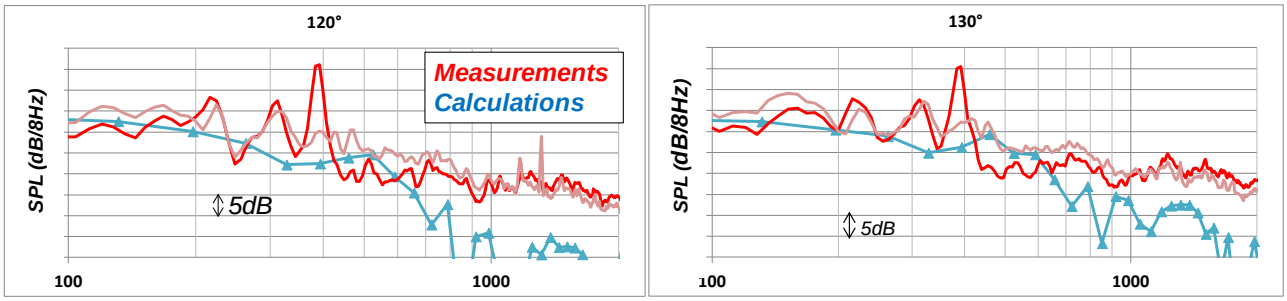

Calculated and measured spectra are very close to each other up to 600Hz. The tonal content is not captured by the simulation, the frequency resolution being too low due to the computation costs of the LES simulation.
This result is found very promising and encouraging for further research.

As a global conclusion for WP4, the application of these new methodologies to full-scale geometries shows that:

- Realistic industrial cases can be handled with these new methods
- Good agreement between calculation and experiments for all configurations
- Direct Combustion Noise generally dominates inside the combustor.
- Indirect Combustion Noise linked with vorticity seems of little importance throughout the propagation path.
- Relative importance of Direct and Indirect combustion noise is test case dependent. This point still remains to be explained.

Weak points of the methodologies used have been identified and tracks for future work explored. Recommendations have been done for better understanding these complex mechanisms.

References

A. Giauque, M. Huet, & F. Clero. (2012). Analytical analysis of indirect combustion noise in subcritical nozzles. *Trans. ASME: J. Engng Gas Turbines Power* .

B. Muhlbauer, B. Noll, & M. Aigner. (1995). Numerical investigation of the fundamental mechanism for entropy noise generation in aero-engines. *Acta Acustica* .

F. Bake, C. Richter, B. Muhlbauer, N. Kings, I. Rohle, F. Thiele, et al. (2009). The Entropy Wave Generator (EWG): A reference case on entropy noise. *Journal of Sound and Vibration* .

F. Marble, & S. Candel. (1977). Acoustic Disturbance from Gas Non-Uniformities Convected Through a Nozzle. *Journal of Sound and Vibration , 55*, 225-243.

I. Duran, S. Moreau, & T. Poinsot. (2013, January). Analytical and Numerical Study of Combustion Noise Through a Subsonic Nozzle. *AIAA Journal* .

J. Lourier, A. Huber, B. Noll, & M. Aigner. (2014). Numerical Analysis of Indirect Combustion Noise Genereation Within a Subsonic Nozzle. *AIAA Journal , 52*.

K. Knobloch, T. Werner, & F. Bake. (2015). Noise Generation in Hot Nozzle Flow.
In: Proceedings of ASME Turbo Expo 2015: Turbine Technical Conference and Exposition. ASME Turbo Expo 2015: Turbine Technical Conference and Exposition, 15.-19.06.2015, Montreal, Canada.

L. Selle, F. Nicoud, & T. Poinsot. (2004). The Actual Impedance of Non-Reflecting Boundary Conditions: Implications for the Computation of Resonators. *AIAA Journal* .

Lax, P. D., & Wendroff, B. (1964). Difference schemes for hyperbolic equations with high order of accuaracy. *Commun. Pure Appl. Math. , 17*, 381-398.

Leyko, M., Moreau, S., Nicoud, F., & Poinsot, T. (2011, January 26). Numerical and anyalitical modelling of entropy noise in supersonic nozzle with a shock. *Journal of Sound and Vibration* .

Smagorinsky, J. (1963). General circulation experiments with the primitive equations: 1. The basic experiment. *Mon. Weather Rev. , 91*.

T. Poinsot, & S. Lele. (1992). Boundary Conditions for Direct Simulations of Compressible Viscous Flows. *Journal of Computational Physics* .

T. Schonfeld, & M. Rudgyard. (1999). Steady and unsteady flows simulations using the hybrid flow solver avbp. *AIAA Journal , 37(11):1378-1385*.